이학석사학위논문

The formation of highly ordered TiO_2 nanotubes array by hard anodization

하드 양극 산화 방법을 이용한 정렬된 타이타니아 나노튜브 합성

2013년 2월

서울대학교 대학원

화 학 부

서 연 주

The formation of highly ordered TiO_2 nanotubes array by hard anodization

하드 양극 산화 방법을 이용한
정렬된 타이타니아 나노튜브 합성

지도교수 이 성 훈
이 논문을 이학석사 학위논문으로 제출함.

2013년 2월

서울대학교 대학원
화학부
서 연 주

서연주의 이학석사 학위논문을 인준함.
2013년 2월

위 원 장 _____ (인)

부위원장 _____ (인)

위 원 _____ (인)

Abstract

The formation of highly ordered TiO_2 nanotubes array by hard anodization

Seo, Yeon Ju
School of Chemistry
The Graduate School
Seoul National University

The regularly ordered valve metal oxide nanotubes can be formed by our well-established electrochemical anodization processes. Among them, the regular arrays of TiO_2 nanotubes are promising candidates for solar energy conversion as a photoelectrochemical cell.

Numerous researchers and technicians have made efforts to increase the growth rate of titania nanotubes by anodization in terms of the control of various parameters. A high applied voltage favors fast nanoporous TiO_2 films but it produces less regular TiO_2 nanotubes. It is not clearly understood how the applied voltage and the electrolyte components have influences on the formation and growth of TiO_2 nanotubes.

In this study, we investigated the relation between an applied voltage and electrolyte condition. The ratio of the molar concentration of ammonium fluoride to water was systematically varied with an applied voltage in

order to prevent 'burning' or 'breakdown' and thus to achieve the fabrication of regular nanotubes array even at an high voltage such as 300 V. The high electric field strength results in the fast growth (1-1.6μm/min) of the array of nanotubes on the surface of the titanium. With an increasing anodization temperature, the thickness of the nanotube walls gets increased due to the acceleration of the oxidation of Ti in the oxide/metal interface. Under the hot electrolyte (56℃) condition, a hexagonal closed packed array of nanotubes were revealed partially on the top of the surface region. Another effort is currently underway to form such a regular and uniform array of zirconium oxide nanotubes.

Key words: *TiO_2 nanotube, hard anodization, electrochemical method*

Student number: 2009-22908

Table of Contents

Abstract..... **i**

Table of Contents..... **iii**

List of Scheme..... **V**

List of Figure..... **Vi**

List of Table..... **Vii**

Chapter 1 Backgrounds and Objective..... **1**

Chapter 2 Introduction..... **6**

Chapter 3 Experimental

3.1 Materials and electropolishing..... **9**

3.2 Anodization..... **9**

3.3 Characterization..... **13**

Chapter 4 Results and Discussion

4.1 Control of the electrolyte composition **14**

4.2 Effect of the temperature..... **22**

4.3 Physical & chemical properties..... **28**

Chapter 5 Conclusions..... **29**

References..... **30**

Abstract (Korean) **34**

Acknowledgements (Korean) **36**

List of Scheme

Scheme 1.1	(a) Typical current–time (j–t) characteristics after a voltage step in the absence (----) and presence (——) of fluoride ions in the electrolyte. (b,c) Schematic drawing showing fieldaided transport of mobile ions through the oxide layers in the absence and presence of fluoride ions.
Scheme 1.2	Schematic diagram for barrier type alumina and porous type.
Scheme 4.1	Schematic diagram of the pore formation.
Scheme 4.2	Scheme showing anode behavior at various potentials.

List of Figure

Figure 3.1	The experimental set-up for electrochemical oxidation. (a) a digital multimeter (34401A, HP) interfaced with a computer and a DC power supply (N5753A model, Agilent) (b) Labview program (c) a well-insulated bath.
Figure 4.1	SEM images of TiO_2 NTs anodized in electrolytic solutions with different concentrations of water.
Figure 4.2	The outer diameter versus. water contents.
Figure 4.3	(a) The molar ratio of NH_4F to water added in an ethlyene glycole-based electrolyte with each applied voltage for self-organized nanotube growth (b) the length of TiO_2 nanotubes grown for 10 min at the each potentail.
Figure 4.4	SEM micrographs of the side view of the TiO_2 nanotube arrays grown on the Ti substrate at (a) 120 V (b) 200 V (c) 300 V and the bottom of nanotubes (d) 120 V (e) 200 V (f) 300 V for 10 min.
Figure 4.5	SEM mictrographs of the side view and the top view of titania nanotubes arrays grown on the pre-patterned titanium substrate at 160 V at (a) 30 ℃ (b) 36 ℃ (c) 46 ℃ in the ethylene glycole based-electrolyte solution with 1.9 M D.I. water and 0.027 M ammonium fluoride for 30 min.
Figure 4.6	SEM micrographs of highly ordered self-organized arrays of TiO_2 nanotubes anodized at 160 V at 56.5 ℃ in the ethylene glycol based electrolyte solution with 1.8 M D.I. water and 0.027 M ammonium fluoride for 30 min. (a) the thickness (b) the arrangements of pores (c) the top parts (d) the bottom parts of the nanotube film (e) current density-time transients.
Figure 4.7	Chemical composition of anodic titania nanotubes at a constant of 50 V and 120 V.
Figure 4.8.	The x-ray diffraction patterns (a) initially-amorphous TiO_2 nanotube and (b) the thermal annealed TiO_2 nanotubular structures anodized at 120 V.

List of Table

Table 4.1 The summary of the anodization condition parameters and results at various applied voltages.

Table 4.2 The summary of the anodization condition parameters and results on a wide range of temperature.

CHAPTER 1. Backgrounds and Objective

Electrochemical oxidation of aluminum was intensively investigated to form protective oxide films on its surface. In particular, anodic porous alumina membrane is one of the most frequently utilized templates to synthesize nanowires or nanotubes with monodisperse diameter and high aspect ratios. [1]

A profound comprehension of the formation mechanism of porous alumina structures prompted increased interests of numerous researchers and technicians in the synthesis of other transition-metal oxide nanostructures by utilizing the anodization technique.

1.1. The mechanism of anodic nanoporous oxide growth

Under the high field approximation, the ionic current density is determined by $X_{barrier}$, the thickness of barrier layer, under a constant polarization by an equation of the form. [2]

$$i = A\exp\left(\frac{\beta\Delta U}{X_{barrier}}\right) \quad (1)$$

where both A and β are constante as temperature- and metal-dependent parameters. The thinning of oxide lead to increase of the ionic current density. The transient of the potentiostatic current density reflects the

type of oxide layer. [3] In the case of the barrier film, the current density j decreases expenentially and decays ultimately as shown in scheme 1.1 (a) On the other hand, in the presence of fluoride in the electrolyte, j decreases exponentially at the 1st mophological stage in scheme 1.1 (a) because of growing non-conductive oxide layer. Afterward, the localized dissolution or thinning of the oxide layer leads to increase of the current density at the 2nd stage in scheme 1.1 (a). Anodic nanoporous oxide film grows on the metal surface when the dissolution rate at the electrolyte/oxide interface is equilibrated with the rate of oxidation at the oxide/metal interface in the 3rd stage in scheme 1.1 (a).

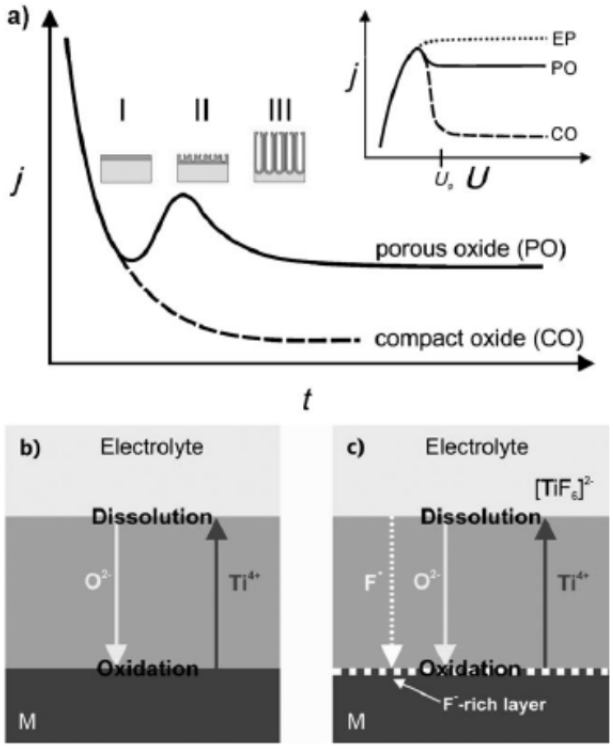

Scheme 1.1 a) Typical current–time (j–t) characteristics after a voltage step in the absence (----) and presence (——) of fluoride ions in the electrolyte. Either compact oxide (fluoride free) or porous/tubular metal oxide formation (containing fluoride) forms by different morphological stages (I–III). The inset shows typical linear sweep voltammograms (j–U curves) for different fluoride concentrations resulting in either electropolished metal (high fluoride concentration), compact oxide (very low fluoride concentration), or tube formation (intermediate fluoride concentration). b,c) Schematic drawing showing fieldaided transport of mobile ions through the oxide layers in the absence and presence of fluoride ions: rapid fluoride migration leads to accumulation at the metal–oxide interface. [4]

1.2. The type of oxide layer on the metal surface

The type of anodic alumina films can be dependent on the solubility of the oxide in an electrolyte.[3] The anodic porous alumina can be realized in soluble electrolytes such as sulfuric, phosphoric, chromic and oxalic acid. Alumina is separated into inner oxide of high purity alumina and an outer oxide layer[3] in both the barrier-type and the porous-type alumina in scheme 1.2. For a titanium substrate, the presence of fluorides in the electrolyte not only enables Ti^{4+} ions at the oxide/electrolyte interface to eject into the electrolyte, but also causes chemical etching of the formed TiO_2 by forming water-soluble $[TiF_6]^{2-}$ species.[2]

$$Ti^{4+} + 6F^- \rightarrow [TiF_6]^{2-} \quad (1)$$

$$TiO_2 + 6F^- + 4H^+ \rightarrow [TiF_6]^{2-} + 2H_2O \quad (2)$$

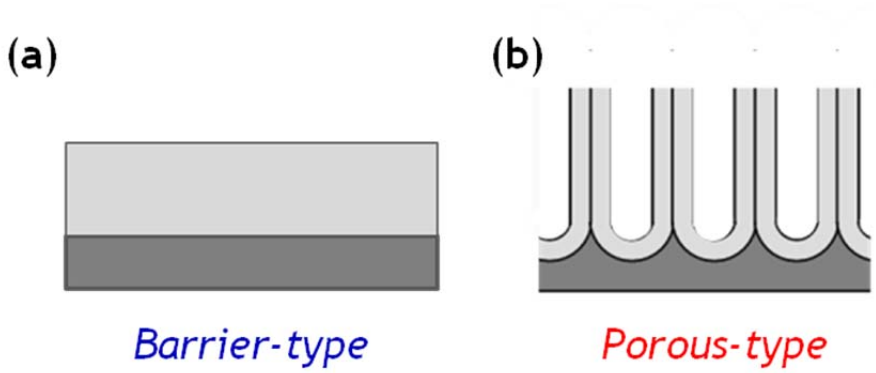

Scheme 1.2 Schematic diagram for barrier type alumina and porous type.

CHAPTER 2. Introduction

For several decades a great attraction has been paid to nanostructures of transition-metal oxide, such as TiO_2,[5-7] ZnO, [8, 9] Al_2O_3, [10-12] ZrO, [13, 14] and Nb_2O_5[15, 16] and their potential applications in various fields. Among these nanostructures, AAO(anodic aluminium oxide) have been most frequently studied for nanotemplate or surface finishing and their findings were recently focused on revealing the mechanism of nanotube formation, [17, 18] which could help to comprehend the growth process of TiO_2 nanotubes on the titanium surface. For AAO, the hard anodization approach has been used for a high-speed fabrication of mechanically robust, very thick and low porosity alumina films.[12] Hard anodization has been generally carried out at a high voltage in order to induce fast growth of Al_2O_3 nanotubes. If this process would be applied to anodization of other transition-metal substrates, the growth rate of the anodic nanotube membranes could be accelerated much more.

The formation of anodic TiO_2 nanotubes was first reported by Zwilling and co-workers in 1999.[19] The TiO_2 nanotubes array formed by electrochemical oxidation of titanium has been extensively investigated

due to unique geometrical structure, facile fabrication process, and its chemical physical characteristics. Anodic TiO_2 nanotubes could be widely utilized for instance in dye-sensitized solar cells[20-23] and hydrogen generators[24, 25]. Recently, several groups succeeded in realization of fast fabrication of anodic TiO_2 nanotube by applying a high potential. Wang et al. first reported on the high growth speed (60 μm/h) of TiO_2 nanotubes by using HF (strong acid) as pore opening reagent.[26] H Yin et al. not only fabricated the self-organized TiO_2 nanotubes with ~600nm outer diameter, but also realized fast growth rate (~100 μm/h).[27] The anodization process was conducted in a high voltage condition by X Yuan et al, and thus a nanotubular structure was formed at 120 V at the maximum rate of 0.97 μm/min.[28] however, there remains one drawback with poor regularity caused by high mechanical stress at the early stage of the anodization and the issue on how the ions ejected from the electrolyte have an influence on anodic TiO_2 nanotube formation has not reach a settlement from electrochemical point of view. Understanding the effects of electrolyte components is particularly crucial for an appropriate control of the anodization condition parameters. Therefore, based on comprehension of the effects of the electrolyte components, this study was aimed of fabrication of anodic titania nanotubes with high regularity and uniformity

even at high anodization potentials. In this paper, hard anodization for titanium foil was carried out at a harsh electrolyte condition, such as a high voltage and a high temperature. As a result, TiO_2 nanotubes with the uniformity of pore size arrangement were formed at from 50 V to 300 V.

Based on the electrochemical knowledge we will keep on studying hard anodization of another valve metal to fabricate more effectively anodic oxide nanotube structures.

CHAPTER 3. Experiment

3.1. Materials and electropolishing

The Ti foil (0.25mm thickness, 99.6% purity, Goodfellow, England) was thoroughly washed by using ethanol and acetone, followed by drying off with N_2 gas. The titanium substrates were electrochemically polished in a mixed solution of perchloric acid(60%), butanol and methanol (1:6:9 in a volume) at 25 V and at -20℃ for 3 min.

3.2. Anodization of the Ti substrate

The mirror-finished titanium substrates were anodized in an ethylene glycol solution containing ammonium fluoride and D.I. water and placed in a well-insulated bath using a dc power supply (N5753A model, Agilent).

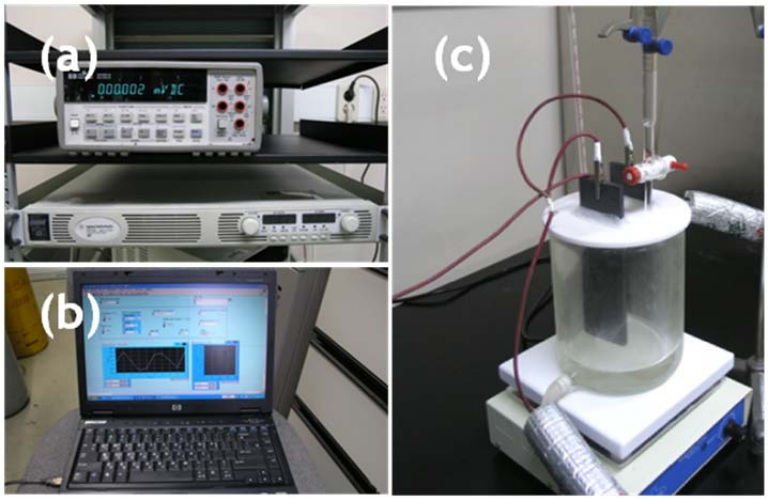

Figure 3.1 The experimental set-up for electrochemical oxidation. (a) a digital multimeter (34401A, HP) interfaced with a computer and a DC power supply (N5753A model, Agilent) (b) Labview program (c) a well-insulated bath.

At the I-II stages, a protective oxide layer with nucleation sites on fluctuations of the surface was formed on the titanium foil at the first anodization potential (E_1) at 20℃ in the ethylene glycol electrolyte with 0.054 M ammonium fluoride for 1 min Then, D.I. water was additionally added in the ethylene glycol based electrolyte containing fluorides. The applied voltage was gradually increased from the first anodization potential (E_1) to the second anodization potential (E_2) at the rate of 0.2-4.0 V/s and then consistently maintained at the second potential (E_2) for 10-30 min. The target voltage ranged from 50 V to 300 V, and the molar ratio

of fluoride to water was changed with the target voltage by adjusting amount of the D.I. water added.

Table 3.1. The summary of the anodization condition parameters and results at various applied voltages.

NH_4F/water (at E_1)	NH_4F/water (at E_2)	$E_1 - E_2$ (V)	sweep rate (Vs^{-1})	Length (μm)
0.049	0.024	60-120	0.2	11
0.049	0.016	50-200	0.5	12
0.024	0.0069	100-300	4	16

Previously we reported on a two step anodization of titanium foil with 30 V in 0.38 wt % NH_4F in ethylene glycol to obtain regular arrays of anodic TiO_2 nanotubes[8]. In this study, the two step anodization process was utilized to anodize Ti foil even in a high temperature at a high voltage. The formed anodic film by anodizing Ti foil over 1 hour at 50 V in the electrolyte with 0.054 M ammonium fluoride and 1.1 M D.I. water (the molar ratio of fluoride to D.I. water is 0.049) was peeled off, and then the

Ti substrate with concave patterns was anodized out at 160 V, changing a temperature from 30 °C to 56 °C.

Table 3.2 The summary of the anodization condition parameters and results on a wide range of temperature.

Temperature (℃)	NH_4F/water (at E_2)	$E_1 - E_2$ (V)	sweep rate (Vs^{-1})
30	0.014	50-160	0.5
36	0.014	50-160	0.5
46	0.014	50-160	0.5
56	0.014	50-160	0.5

Finally, the fabricated TiO_2 nanotube arrays were thermally annealed at 450 ℃ for 2 h with a heating rate of 1.7 ℃·min^{-1} in an ambient condition.

3.3. Characterization

The anodization current was monitored with time using a digital multimeter (34401A, HP) interfaced with a computer. The morphological characterization of the samples was done by a field-emission scanning electron microscope (SUPRA 55VP, Carl Zeiss). The crystal structure was identified by x-ray diffractometer(D5005, Bruker) using a monochromatic Cu Kα radiation (λ = 1.54 Å) in the 2Θ angle range of 20° to 60°.

CHAPTER 4. Results and Discussion

4.1. Control of the electrolyte composition

Under the high field theory, the ionic current is exponentially proportional to the anodization potential, and thus the oxide nanotube growth rate generally increases with the applied voltage. [2]

$$i = A\exp\left(\frac{\beta\Delta U}{x_{barrier}}\right) \quad (1)$$

However, only controlling an applied potential is not enough to accomplish both high speed growth and highly ordered nanotubes arrays at a time.

The process of anodic nanotubes growth can be divided the four stages. In the I-II anodization stages, the titania layer is grown on the surface of Ti substrate, and the orandomly formed etching pits with the presence of fluroride develop into the pore nucleation sites. In the III-IV anodization stages, the oxidation growth rate of the Ti metal at the oxide/metal interface is balanced with the chemical etching rate of the oxide through fluoride at the oxide/electrolyte interface.

$$Ti^{4+} + 6F^{-} \rightarrow [TiF_6]^{2-} \quad (1)$$

$$TiO_2 + 6F^{-} + 4H^{+} \rightarrow [TiF_6]^{2-} + 2H_2O \quad (2)$$

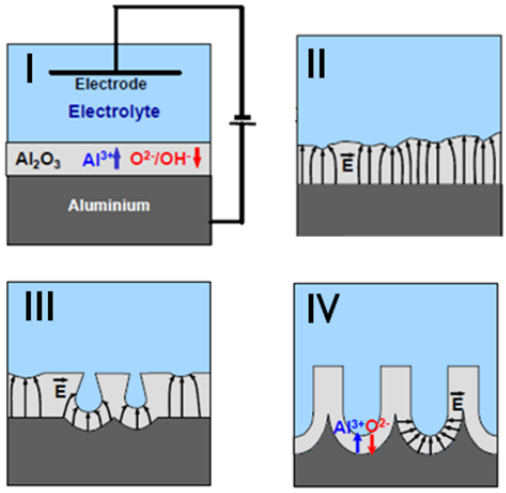

Scheme 4.1 schematic diagram of the pore formation[3]

I-II stages proceed in a relatively low voltage to create a protective layer with the pore nucleation sites. Afterward, the III-IV anodization stages for the oxide growth, acceleration of the growth rate of the oxide film is realized by a high electric field.

Excess fluorides as etching species trigger ‘burning’ or ‘breakdown’ at a high applied voltage. In this study, the molar ratio of fluoride to water is controlled to prevent the mophological catastropic events.

In terms of anions, fluorides compete with hyrdoxides ejected from water molecules in the electrolyte/oxide interface by an electric field. When increasing the amount of water involved in the electrolyte, the etching rate of the oxide is retarded. As a result, nanotubes with thicker walls are grown on the surface of the Ti substrate. To confirm the influence of the relative concentration of fluoride to water molecule, the amount of water in the electrolyte was only controlled with the concentration of the fluoride in constant. As shown in figure 4.1, the outer diameter increases with the increase of water contents. This is attributed to the increaed wall thickness due to the redarded etching rate of the oxide.

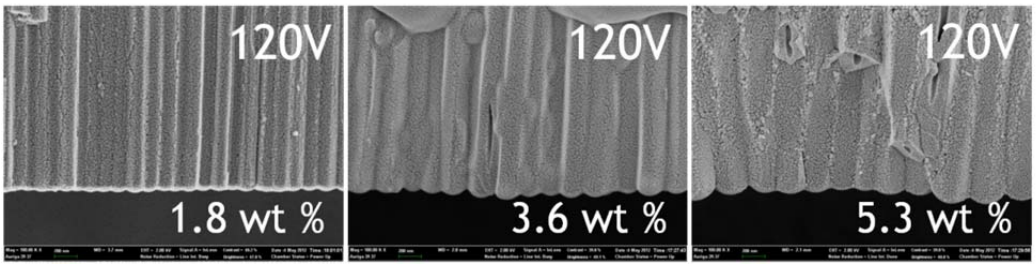

Figure 4.1 SEM images of TiO_2 NTs anodized in electrolytic solutions with different concentrations of water

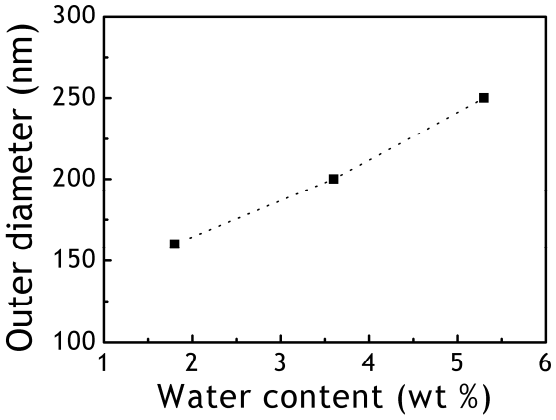

Figure 4.2 The outer diameter versus. water contents

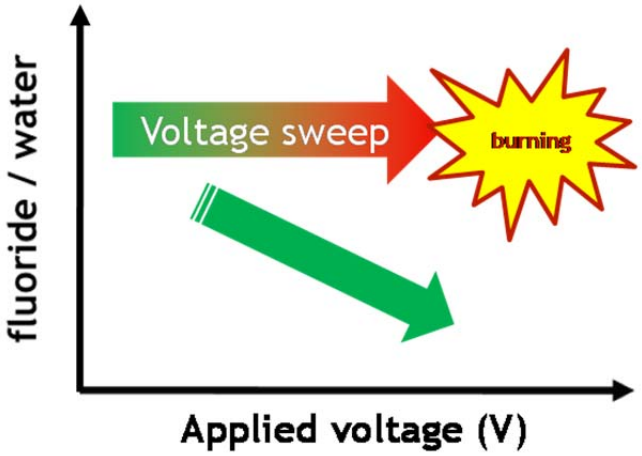

Scheme 4.2. Scheme showing anode behavior at various potentials.

The molar ratio of NH_4F to D.I. water involved in the ethylene glycol-based electrolyte need to decreas with increase of the applied potential at the high applied potential to reduce activities of the fluorides. (Scheme 4.2)

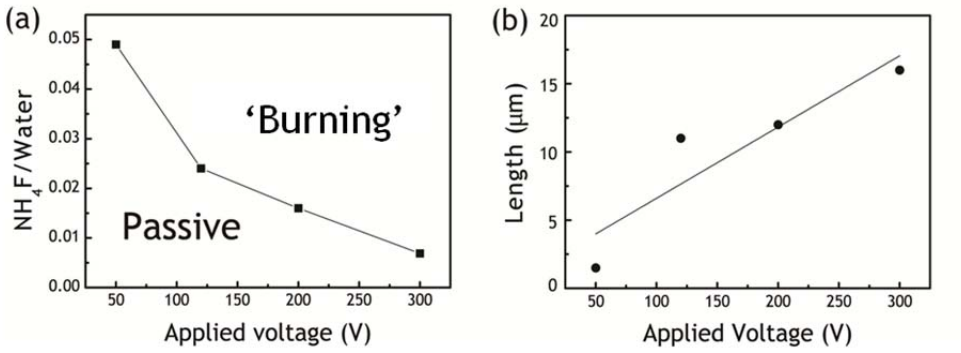

Figure 4.3. (a) The molar ratio of NH_4F to water added in an ethlyene glycole-based electrolyte with each applied voltage for self-organized nanotube growth (b) the length of TiO_2 nanotubes grown for 10 min at the each potentail.

After initiating the randomly distributed nucleation centers in a thin oxide layer for 1 min in mild condition (50 V), the water was additionally injected to decrease the ratio of fluoride to water, and then the voltage is gradually increased to the target high voltage at the rate of 0.2-4.0 V/s and finally maintained at the final voltage for 10 min.

Figure 4.3 (a) shows the molar ratio of NH_4F to water added in ethlyene glycol-based electrolyte with each applied voltage to induce self-organized nanotube growth on the surface of the substrate. It was confirmed that the additionally supplied water moelcules in the electrolyte prevents the 'breakdown' or 'burning', which can induce mopological catastrophic events. The surface morphologies of anodic TiO_2 films were investigated at 120-300 V in ethylene glycol containing the molar ratio of NH_4F to water at each voltage at 20 °C (figure. 4.4).

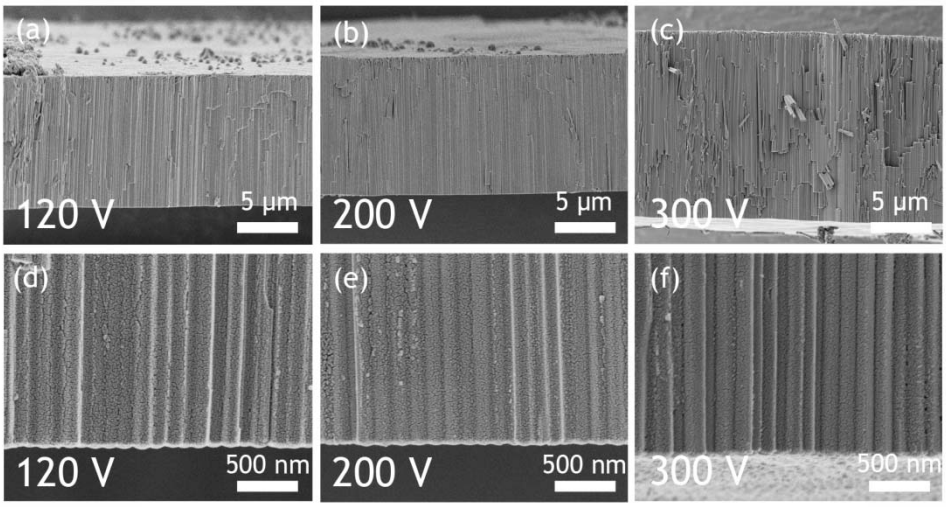

Figure 4.4. SEM micrographs of the side view of the TiO_2 nanotube arrays grown on the Ti substrate at (a) 120 V (b) 200 V (c) 300 V and the bottom of nanotubes (d) 120 V (e) 200 V (f) 300 V for 10 min.

As a result, regular array of titania nanotubes was produced on the titanium surface even at an extremely high voltage, such as 300 V. Also, it is proven that the length of anodic TiO_2 nanotubes for 10 min gradually increases with the applied voltage, from 50 V to 300 V. (figure 4.3 b).

As shown in figure 4.4, the outer diameters (145nm) of nanotubes anodized at each voltage are approximately similar to each other, the values are relatively smaller than that of anodic TiO_2 nanotubes grown at a high potential reported at other groups. This might be attributed to the application of a mild voltage (50 V) at the I-II anodization stages.

4.2. Effect of the temperature

Figure 4.5 shows three kinds of highly self-organized anodic TiO_2 nanotubes grown in ethylene glycol containg H_2O (1.9 M) and NH_4F (0.027 M) at 30, 36 and 46 °C for 30 min (using concave-patterned Ti foil in the second anodization step) by the two step anodization.

In the second anodization step, the pre-patterned periodic concaves make the electric field concentrated at their centers and acts as pore nucleation centers. Since the regular nucleation centers are already arranged in the early stage of the nanotube growth, highly ordered nanotubes array was produced even at 160 V even in a high temperature. As the anodization temperature increases, hexagonal closed packed arrangement of pores appeared. Also, the pore size of the top view of titania nanotubes decreases as the temperature increases. This is because the oxidation of Ti at the oxide/metal interface is accelerated and the wall of the oxide is thicker.

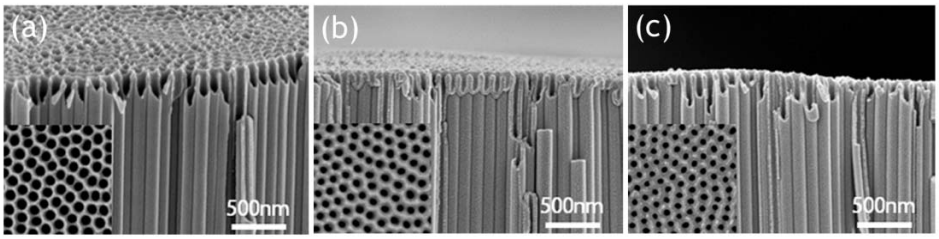

Figure 4.5. SEM mictrographs of the side view and the top view of titania nanotubes arrays grown on the pre-patterned titanium substrate at 160 V at (a) 30 ℃ (b) 36 ℃ (c) 46 ℃ in the ethylene glycole based-electrolyte solution with 1.9 M D.I. water and 0.027 M ammonium fluoride for 30 min.

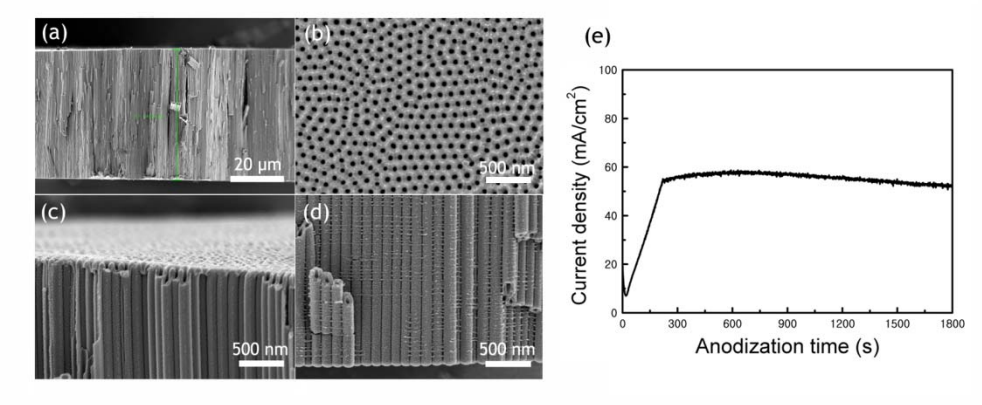

Figure 4.6. SEM micrographs of highly ordered self-organized arrays of TiO_2 nanotubes anodized at 160 V at 56.5 ℃ in the ethylene glycol based electrolyte solution with 1.8 M D.I. water and 0.027 M ammonium fluoride for 30 min. (a) the thickness (b) the arrangements of pores (c) the top parts (d) the bottom parts of the nanotube film (e) current density-time transients

As expected, the top surface of nanotubes no had debris or collapsed bundles of oxide in the top view of self-organized TiO_2 nanotubes, (figure. 4.6b) The regular and uniform arrays of pores were confirmed on the top view of anodic TiO_2 nanotubes and the pore diameter was relatively smaller than that of anodic TiO_2 nanotubes grown at a high anodization potential reported at other groups due to the first anodization step.[14-16] This relatively small diameter has an advantage in applications as photovoltaic devices in terms of the large surface area. According to the microscopic analysis, the 30-50 μm anodic TiO_2 film was grown on the surface of the Ti substrate for 30min. (figure. 4.6a) High speed growth was achieved by the high voltage and temperature, although the amounts of ammonium fluoride seem insufficient in the electrolyte in Table 3.2. As shown in figure 4.6.(c)-(d), the outer diameter of the tube is maintained unchanged along the tube from the surface to the bottom.

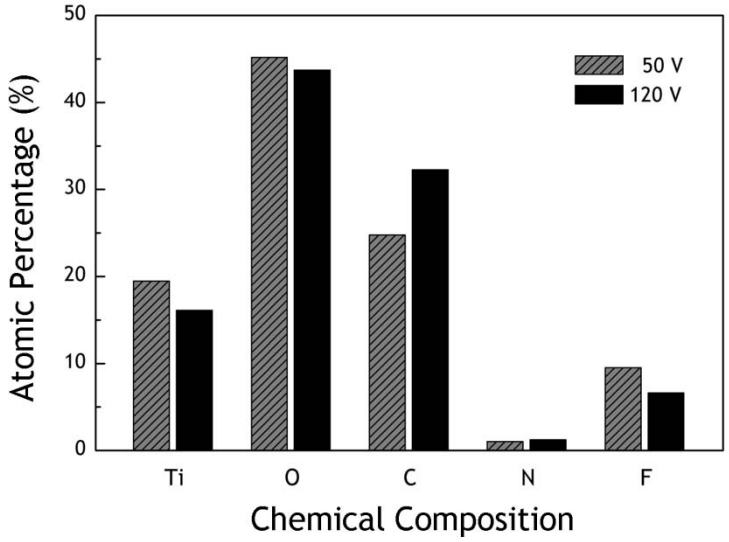

Figure 4.7. Chemical composition of anodic titania nanotubes at a constant of 50 V and 120 V

As shown figure 4.7, as-formed nanotubes contain significant amounts of impurities , such as carbons, nitrogens, and fluorides. The atomic percentage of carbon is richer in the anodic oxide grown at 120 V than 50 V. Inversely, the percentage of fluoride is poor in the nanotube formed at a constant of 120 V.

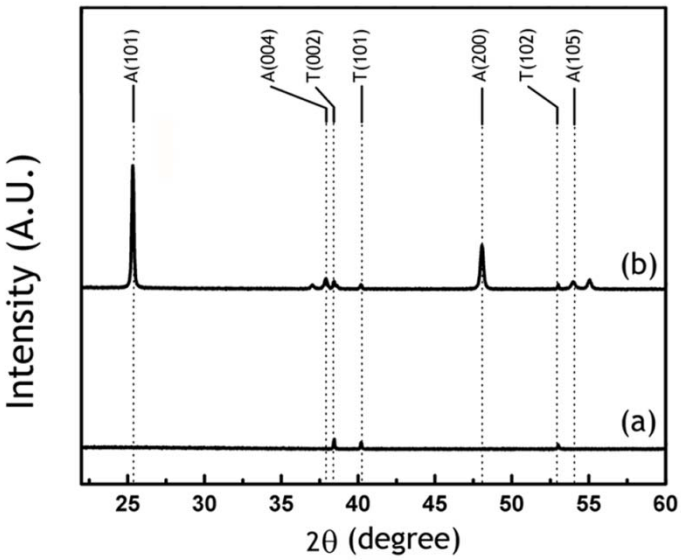

Figure 4.8. The x-ray diffraction patterns (a) initially-amorphous TiO_2 nanotube and (b) the thermal annealed TiO_2 nanotubular structures anodized at 120 V.

The as-prepared TiO_2 nanotubes are initially amophorous in nature and the TiO_2 membrane with anatase structure was obtained by annealing amorphous TiO_2 at 450℃ for 2 hours in an ambient condition. The XRD patterns of initially-amorphous TiO_2 nanotube and the thermal annealed TiO_2 nanotubular structures show the specific peaks. (figure 4.8)

CHAPTER 5. Conclusions

Hard anodization enables high speed fabrication of nanoporous oxide films, while there is the problem concerning poor regularity. In this study, it is crucial to form a protecting layer by mild anodization or use concave patterned Ti substrates in I-II stages. Afterward, in III-IV stages, with increase of the applied voltage, the concentration of additives (NH_4F and water) in an ethylene glycol-based electrolyte was varied to prevent the morphological catastrophic events. As a result, highly regular and well ordered TiO_2 nanotube oxide films were successfully fabricated at various anodization voltages from 50V to 300V.

References

1. Wang, X.; Wang, X.; Huang, W.; Sebastian, P. J.; Gamboa, S., Sol–gel template synthesis of highly ordered MnO2 nanowire arrays. *Journal of Power Sources* 2005, *140*, 211-215.

2. Prakasam, H. E.; Shankar, K.; Paulose, M.; Varghese, O. K.; Grimes, C. A., A New Benchmark for TiO2 Nanotube Array Growth by Anodization. *The Journal of Physical Chemistry C* 2007, *111*, 7235-7241.

3. die, g. d., FABRICATION OF MONODOMAIN POROUS ALUMINA USING NANOIMPRINT LITHOGRAPHY
AND ITS APPLICATIONS. *zur Erlangung des akademischen Grades Doktoringenieur (Dr.-Ing.) Dissertation* 2004.

4. Roy, P.; Berger, S.; Schmuki, P., TiO2 Nanotubes: Synthesis and Applications. *Angewandte Chemie International Edition* 2011, *50*, 2904-2939.

5. Dawei Gong; Craig A. Grimes; Oomman K. Varghese; Wenchong Hu; R. S. Singh; Dickey, Z. C. a. E. C., Titanium oxide nanotube arrays prepared by anodic oxidation. *Journal of Materials Research* 2001, *16*, 3331-3334.

6. Karthik, S.; Gopal, K. M.; Haripriya, E. P.; Sorachon, Y.; Maggie, P.; Oomman, K. V.; Craig, A. G., Highly-ordered TiO 2 nanotube arrays up to 220 μm in length: use in water photoelectrolysis and dye-sensitized solar cells. *Nanotechnology* 2007, *18*, 065707.

7. Grimes, C. A., Synthesis and application of highly ordered arrays of TiO2 nanotubes. *Journal of Materials Chemistry* 2007, *17*, 1451-1457.

8. Becheri, A.; Dürr, M.; Lo Nostro, P.; Baglioni, P., Synthesis and characterization of zinc oxide nanoparticles: application to textiles as UV-absorbers. *Journal of Nanoparticle Research* 2008, *10*, 679-689.

9. Jones, N.; Ray, B.; Ranjit, K. T.; Manna, A. C., Antibacterial activity of ZnO nanoparticle suspensions on a broad spectrum of microorganisms. *FEMS Microbiology Letters* 2008, *279*, 71-76.

10. Masuda, H.; Fukuda, K., Ordered Metal Nanohole Arrays Made by a Two-Step Replication of Honeycomb Structures of Anodic Alumina. *Science* 1995, *268*, 1466-1468.

11. Nielsch, K.; Choi, J.; Schwirn, K.; Wehrspohn, R. B.; Gösele, U., Self-ordering Regimes of Porous Alumina: The 10 Porosity Rule. *Nano Letters* 2002, *2*, 677-680.

12. Lee, W.; Ji, R.; Gosele, U.; Nielsch, K., Fast fabrication of long-range ordered porous alumina membranes by hard anodization. *Nat Mater* 2006, *5*, 741-747.

13. Tsuchiya, H.; Macak, J. M.; Ghicov, A.; Taveira, L.; Schmuki, P., Self-organized porous TiO2 and ZrO2 produced by anodization. *Corrosion Science* 2005, *47*, 3324-3335.

14. Yeonmi, S.; Seonghoon, L., A freestanding membrane of highly ordered anodic ZrO 2 nanotube arrays. *Nanotechnology* 2009, *20*, 105301.

15. Gomes, M. A. B.; Bulhoes, L. O. d. S.; de Castro, S. C.; Damiao, A. J., The Electrochromic Process at Nb[sub 2]O[sub 5] Electrodes Prepared by Thermal Oxidation of Niobium. *Journal of The Electrochemical Society* 1990, *137*, 3067-3070.

16. Choi, J.; Lim, J. H.; Lee, S. C.; Chang, J. H.; Kim, K. J.; Cho, M. A., Porous niobium oxide films prepared by anodization in HF/H3PO4. *Electrochim. Acta* 2006, *51*, 5502-5507.

17. Houser, J. E.; Hebert, K. R., The role of viscous flow of oxide in the growth of self-ordered porous anodic alumina films. *Nat Mater* 2009, *8*, 415-420.

18. Hebert, K. R.; Albu, S. P.; Paramasivam, I.; Schmuki, P.,

Morphological instability leading to formation of porous anodic oxide films. *Nat Mater* 2011, *advance online publication*.

19. Zwilling, V.; Aucouturier, M.; Darque-Ceretti, E., Anodic oxidation of titanium and TA6V alloy in chromic media. An electrochemical approach. *Electrochim. Acta* 1999, *45*, 921-929.

20. Kongkanand, A.; Tvrdy, K.; Takechi, K.; Kuno, M.; Kamat, P. V., Quantum Dot Solar Cells. Tuning Photoresponse through Size and Shape Control of CdSe−TiO2 Architecture. *Journal of the American Chemical Society* 2008, *130*, 4007-4015.

21. Wang, J.; Lin, Z., Dye-Sensitized TiO2 Nanotube Solar Cells with Markedly Enhanced Performance via Rational Surface Engineering. *Chemistry of Materials* 2009, *22*, 579-584.

22. Jennings, J. R.; Ghicov, A.; Peter, L. M.; Schmuki, P.; Walker, A. B., Dye-Sensitized Solar Cells Based on Oriented TiO2 Nanotube Arrays: Transport, Trapping, and Transfer of Electrons. *Journal of the American Chemical Society* 2008, *130*, 13364-13372.

23. Mor, G. K.; Shankar, K.; Paulose, M.; Varghese, O. K.; Grimes, C. A., Use of Highly-Ordered TiO2 Nanotube Arrays in Dye-Sensitized Solar Cells. *Nano Letters* 2005, *6*, 215-218.

24. Mor, G. K.; Shankar, K.; Paulose, M.; Varghese, O. K.; Grimes, C. A., Enhanced Photocleavage of Water Using Titania Nanotube Arrays. *Nano Letters* 2004, *5*, 191-195.

25. Park, J. H.; Kim, S.; Bard, A. J., Novel Carbon-Doped TiO2 Nanotube Arrays with High Aspect Ratios for Efficient Solar Water Splitting. *Nano Letters* 2005, *6*, 24-28.

26. Wang, D.; Liu, Y.; Yu, B.; Zhou, F.; Liu, W., TiO2 Nanotubes with Tunable Morphology, Diameter, and Length: Synthesis and Photo-Electrical/Catalytic Performance. *Chemistry of Materials* 2009, *21*, 1198-1206.

27. Yin, H.; Liu, H.; Shen, W. Z., The large diameter and fast growth of self-organized TiO 2 nanotube arrays achieved via electrochemical anodization. *Nanotechnology* 2010, *21*, 035601.

28. Xiaoliang, Y.; Maojun, Z.; Li, M.; Wenzhong, S., High-speed growth of TiO 2 nanotube arrays with gradient pore diameter and ultrathin tube wall under high-field anodization. *Nanotechnology* 2010, *21*, 405302.

국문초록

균일하게 정렬된 밸브 금속 산화물의 나노튜브 구조체는 본 연구진의 전기화학적 산화 방법 기술로 합성이 가능하다. 밸브 금속 산화물 중에서 균일하게 정렬된 타이타니아 나노튜브 구조체는 전기화학 셀에서 태양광 에너지 변환 시스템을 위한 전극으로서 각광받고 있는 후보 물질이다.

전기화학적 산화방법을 통하여 나노튜브의 구조 파라미터를 제어하고 산화물의 성장 속도를 증가 시키기 위한 연구가 많은 과학자들과 기술자들에 의해 진행되어져왔다. 지금까지 확립된 이론에 따라 전압은 타이타니아 나노튜브 필름의 성장 속도를 증가 시킬 수 있다는 것을 실험적으로 증명해 왔지만, 높은 전압에서 길어진 나노튜브 구조체의 경우 낮은 전압에서 길러진 경우와 비교하였을 때 빠른 성장속도에 의하여 구조체의 균일성이나 규칙성이 현격하게 떨어지는 단점이 있었다. 또한 전압과 전해질에 첨가되는 음이온이 산화물 형성과 성장에 어떻게 영향을 미치는지 명확히 밝히지 못했기 때문에 최대로 인가할 수 있는 전압이 200V를 넘지 못했다.

본 연구에서는 이틸렌글리콜에 첨가되는 암모니움 플루오라이드(NH4F)와 물의 몰 비를 조절하면서 높은 전압에서 균일성을 유지할 수 있는 반응 조건을 찾았으며 전압에 따라 첨가되어져야 하는 암모니움 플루오라이드(NH4F)의 양을 예상할 수 있도록 그래프로 나타내었다. 이러한 경향성에 따라서 높은 전압 (300 V)에서도 균일한 나노튜브를 10분 내에 수십 마이크로의 타이타니 나노튜브 필름 합성에 성공하였다. (1-1.6μm/min)

온도가 산화물의 생성 속도를 증가시킨다는 사실을 기반으로 반응 온도를 증가 시킬에 따라서 나노튜브 벽이 두꺼워지면서 포어 사이즈가 작아진다. 높은 온도(56℃)에서도 육방밀집구조의 구조가 부분적으로 형성되었다.

이러한 전압과 온도에 따른 산화전극 성질에 대한 이해를 바탕으로 지르코니아의 균일하고 규칙적인 배열을 갖는 나노구조체 산화물의 성장 속도 제어에 대한 연구를 진행 중에 있다.

주요어 :*타이타니아 나노튜브, 하드 양극산화, 전기화학적 방법*

학번: 2009-22908

감사의 글

지금의 이 자리까지 나를 인도해주신 하나님 감사합니다. 당신의 계획하심과 인도하심 속에서 자라게 해 주셔서 감사합니다.

석사과정을 무사히 마무리하고 또 다른 세계를 향한 발돋움을 할 수 있도록 저에게 도움을 주셨던 모든분들께 감사의 말씀을 전하고 싶습니다. 먼저는 학자로서 뿐만 아니라 인생의 스승으로서 진심어린 삶의 교훈과 자세에 대해 좋은 가르침을 주시고 실험실 생활 통하여 앞으로 삶을 이기고 나갈 좋은 밑거름을 만들 수 있도록 믿고 기다려주신 이성훈 교수님께 깊은 감사를 드립니다. 또한 함께 학위 논문 심사로 수고해 주신 서정쌍 교수님과 강헌 교수님께도 감사드립니다. 석사 과정 동안에 배운 것들을 더 갈고 닦아서 더 빛나고 유용한 지식으로 사회에 이바지 할 수 있는 사람이 되겠습니다.

또한, 실험실 식구들 너무너무 감사하고 보고 싶습니다. ^^ 750번 버스 선배 정표오빠 덕분에 제가 실험실에 들어와서 여지껏 버티고 있어요. 항상 편안함과 위트로 힘들 때마다 마음의 짐을 덜어주셔서 감사합니다. 예슬이를 사랑하는 애영언니, 지금은 사회인으로서 힘차게 살아가는 언니의 모습을 그려봅니다. 포기하지 않고 끝까지 언니의 몫을 해내는 모습 너무 멋있었습니다. 동갑내기 친구이자 실험실 선배로 힘든 일 마다하지 않고 본을 보여준 주현이 모습 고마웠어. 더 마음 나누지 못한 아쉬움 있지만 앞으로 사회에서 더 좋은 모습으로 살아가길 응원할께. 나와 음식 코드도 비슷하고 따뜻한 배려심으로 친동생처럼 잘 챙겨준 수정언니도 정말 많이 고마워요. 언니는 진짜 따뜻하고

멋진 사람이에요. 늘 편한 마음으로 대할 수 있었던 성권 선배님도 고마워. 지금은 다른 길을 걷고 있지만 힘든 학업 잘 마무리하고 멋진 의사쌤이 되길 바래. 늘 내 옆자리에서 내 얘기 많이 들어주고 동감해주고 내 편이 되어준 고운이 지구에서 관악캠퍼스를 뺀 만큼 사랑해 ^_^ 언제나 힘들 때 연락해. 맛있는거 먹으며 아픔도 기쁨도 함께 나누자. 내 왼쪽 옆자리에서 박사과정 하며 늘 바빴지만 저의 심심한 말장난 받아주며 따뜻하게 챙겨준 재훈오빠 감사해요. 임박사님, 화이팅입니다~!! 종종.. 실험실에 찾아오셔서 맛있는거 사주시고 좋은 격려와 조언을 나누어 주신 형윤박사님께도 감사드립니다. 마지막 실험이 후배가 되어준 병권이에게도 고마워. 처음과 같은 마음 변치 말고 석박사 과정 동안에 많이 배우고 성장하길 바라며 기도할게.

HY-SNU 라인들께도 감사의 말씀드려요. 특별히 한양대 05학번 후배 수연이, 언제나 밝은 미소 담고 있는 수연이가 있어서 정말 힘이 되었어~~ 사랑해~~あいしてる~~ I love you~~ Je t'aime~~ ^_^ 예수님, 수연이 항상 보살펴 주시고 어디가서든지 좋은 사람 만날 수 있게 도와주세요~!! 매 학기 마다 맛있는 꼬기도 많이 사주고 챙겨주신 준상오빠 감사해요. 오빠는 진짜 멋진 신랑 멋진 남편이 될꺼에요~!! 04학번 동기 지희~ 박사과정 동안 많이 배우고 성장하길 바라고 기대해. 항상 믿음 위에서 삶을 아름답게 건축해 가길 응원하며 기도할게. HY-SNU 막내둥이 순규. 옆에 있기만 해도 든든한 순규야. 석사과정 잘 마무리하고 인생의 한 단계마다 전적인 주님의 은혜와 사랑이 넘치길 기도할게. 사회에 나가서 선한 영향력을 끼칠 수 있는 멋진 사람이 되어

~!! 화이팅~!!

언제나 해맑고 순수한 아란이~ ^_^ 함께 하는 시간만으로도 감사했어. 앞으로 인생 가운데 어려움 없이 좋은 만남과 축복이 넘쳐나길 기도할게. 졸업하고도 자주 보자~!! 더 많은 시간 함께 하지 못해 아쉬운 혜려. 그냥 혜려의 존재가 나에게는 축복이야. 혜려를 보면 나도 웃게되거든 ^_^ 논자시 시험 멋있게 패스해!! 응원할게~!! 푸들 닮은 귀여운 영진이~ 마지막까지 응원해주고 싶었어~!! 시련과 역경 꼭~ 이겨내고 졸업장 받는 그날까지 파이팅~!!! 센스 넘치는 인혜 함께 했던 일본여행 정말 잊지 못할거야, 주님의 인도하심 따라 오늘 하루도 승리하길 기도할게. 지금은 다른 길을 가고 있지만 각자의 길을 서로 응원해주는 사이인 울림이~ 우리의 목표알지? Doctor가 되는 그날까지 열심히 뛰자~~!!!

벌써 10년지기 친구이자 차차기 CEO감 정윤이, 내가 너 엄청 좋아하고 사랑하는거 알지? 대학 캠퍼스에서 널 만난건 나에게 정말 행운이었어. 너에게 좋은 점들 많이 배우고 너의 섬김이 힘들 때마다 나에게 얼마나 큰 힘과 위로가 되었는지 몰라. ^_^ 늘 솔직하고 담백한 우리의 대화를 즐길 수 있어 만날 때 마다 유쾌함과 즐거움을 선사하는 정은이, 우리의 시시콜콜한 이야기 속에서 주님의 예비하심과 위로하심을 느껴져도 뒤돌아서면 다시 보고 싶어져~ ^_^ 평생 믿음의 동역자로 함께 지내자. C.C.C.에서 새내기 시절 만난 지금은 절친 준호, 네가 새내기 시절 함께 했던 시간들과 이야기들이 이제는 추억이 되었네. 언제나 목표를 향해 자신을 부지런히 가꾸는 네 모습 멋있고 앞으로

주님의 너를 쓰실 일 기대가 되어. 내가 엄청 좋아하고 존경하는 미화 순장님, 순장님의 앞 길을 응원합니다. 우리 앞으로 열심히 연습해서 네이티브랑 자연스럽게 대화하는 그날을 꿈꿔요. 예쁜 순원 지은이, 대학시절 심심한 나를 늘 유쾌하게 만들어준 지은이가 기억나. 이제는 사회인으로서 힘든 일 많겠지만 잘 이겨내고 우리 주님 사랑 안에서 서로 위로하며 격려하며 많은 시간 함께 하기로 약속하자~!!

섬세함과 배려심 많은 유리~ 내가 엄청 사랑하는거 알지? 언제나 네 삶을 축복하고 응원할게~!! 우리 자주보자~ 내가 연락 많이 할게 ^_^ 상큼하고 발랄한 민정이 함께 해줘서 그동안 고마웠고 앞으로도 좋은 만남 계속 이어가자. 배려심 깊고 신중한 선아, 앞으로도 언제나 그 모습 변치 말고 사회에서 좋은 영향력을 끼치는 사람이 되길 기도할게~ ^_^

세상에서 가장 존경하는 샛별교회 정상신 목사님과 최은혜 사모님. 제가 지구 어디에 있어도 두 분의 은혜는 잊지 못할 겁니다. 그래서 평생 두분께 받은 은혜와 사랑을 기억하며 다른 사람에게 베풀 수 있는 사람이 되도록 노력할게요. 사랑합니다. 샛별교회 청년회 식구들 감사하고 사랑합니다.

내가 세상에서 가장 사랑하는 엄마, 아빠. 두 분이 내 곁에 있어서 얼마나 큰 빽인지 몰라요. 항상 감사하고 존경하고 사랑했습니다. 저는 두분께 너무 벅찬 사랑을 받았습니다. 그리고 항상 정직하고 착한 마음으로 살아주셔서 감사했습니다. 이런 두 분의 모습이 저를 살게하고 제가 어긋나지 않고 저의 길을 걸어갈 수 있는 가장 큰 힘이었습니다. 정말 많이 사랑합니다. 항상 맛있

는거 사주고 내 부탁 잘 들어준 쌍둥이 남동생 민기, 만기에게도 정말 고마워. 너희들의 삶에도 주님의 은혜가 넘쳐나길 기도할게. 너희는 정말 멋진 사람이 될거야.